USING AN AUTOMATED CRATER DETECTION ALGORITHM AS A TOOL FOR MAPPING SECONDARY CRATER CLUSTERS ON THE MOON: CHANG'E 5 LANDING SITE.

J. H. Fairweather[1], A. Lagain[1], K. Servis[1,2], G.K. Benedix[1,3,4], and P.A. Bland[1,2]. [1]School of Earth and Planetary Sciences, Curtin University, GPO Box U1987, Perth, WA, 6845, Australia, [2]CSIRO, Pawsey Supercomputing Centre, Kensington, WA, 6151, Australia, [3]Department of Earth and Planetary Sciences, Western Australia Museum, Locked Bag 49, Welshpool, WA 6986, Australia, [4]Planetary Science Institute, 1700 East Fort Lowell, Suite 106, Tuscon AZ 85719-2395, USA, (john.fairweather@postgrad.curtin.edu.au).

Introduction: The Moon has been subject to a host of sample return missions (Apollo 11, 12, 14, 15, 16, 17; Luna 16, 20, 24; and now Chang'E 5), where these rare samples have greatly aided in our understanding of the lunar surface [1,2,3]. A question for some components within the collected samples (particularly soil samples) is where exactly does the material originate from and what particular impact influenced their formation [1,4]. Small glass spherules, for example, can be formed and transported through impacts, some of these transported components are contained within the collected lunar soil samples. The spherules capture and contain significant information (age and composition) about the impact event that transported them, therefore the ability to determine where they come from gives us information about unvisited impact sites [3,5]. The impact crater population smaller than 1 km is largely contaminated by secondary craters, which form from falling material ejected during an impact, and if the ejected debris is large enough it will form small impact craters [4,6]. These types of craters tend to form in clusters or rays radiating away from the primary impact crater. Looking at impact craters at any scale, we can compute crater densities to aid in identifying clusters of secondary craters that can be linked to a larger primary crater [5,6]. Generating these datasets down to a ~100m scale is required to create detailed maps of secondary crater clusters, which is tedious and time consuming. Here we show how an automated crater detection algorithm can aid in identifying clusters and greatly reduce the time-consuming aspects of generating a small crater dataset. Using the highest resolution lunar imagery, the Lunar Reconnaissance orbiter – Narrow Angle Camera (LRO-NAC) offering a resolution of 0.5-2 m/px [7], we can automatically detect craters down to ~20-30m. We chose to focus on the Chang'E 5 landing site, which successfully completed a sample return, we have trained and run our Crater Detection Algorithm (CDA) over a mosaic of LRO-NAC images, from which we have compiled a 3.9 million crater dataset. Sample providence analyses have been conducted across this site using a host of techniques and methods such as numerical modelling, where likely candidates for ejecta material was identified [3]. Additional methods and datasets, such as the CDA, will compliment and aid in determining secondary clusters.

The Crater Detection Algorithm and the NAC Dataset: The CDA is a Convolutional Neural Network running through an adapted version of 'You Only Look Once version 3' (YOLOv3) as the network's architecture [8]. YOLOv3 specializes in ultra-fast object detection across an image-based dataset. The detection model we use for YOLOv3 is trained and validated across 247 square NAC image tiles (416 pixels in length/width). Within those tiles are 43,402 manually marked craters, ranging from 2m to 400m. All the image tiles have afternoon/morning lighting conditions (incidence angle range of 45°-82°), to facilitate impact crater recognition. The LRO-NAC dataset, at 0.5-2m/px resolution, gives the opportunity to detect deca-meter sized craters across large areas of the lunar surface. Before running the detection model across the NAC images, they are processed and converted into GeoTiffs through USGS ISIS3 and GDAL, respectively [9]. The 450,000km by 275,000km mosaic was created via stitching together 871 pre-processed NAC images at a downgraded resolution of 5m/px. We chose to make a downsampled single NAC mosaic, instead of running the CDA across the individual NAC images, to help mediate the NAC image offsets remove the chance of overlapping detections. The mosaic covers the northern Oceanus Procellanum region and the Chang'E 5 site.

Performance of the CDA: This lunar detection model, was adapted and retrained from an existing Martian detection model [10,11]. The lunar CDA has a recall (True Positive rate) of 0.91 (91%) across NAC images with good sunlight conditions (morning or evening lighting) and is suitable for detecting fresh to moderately degraded impact craters across mare and highland terrains [12,13].

Chang'E 5 Landing Site: We ran our crater detection model over the northern Oceanus Procellanum mosaic, the total area of roughly 100,000 km^2. Our model detected 3.9 million craters with a diameter range of 33m to 2.1 km. The detection process took ~35 minutes to complete on the Topaz supercomputer at Pawsey Supercomputing Centre, Perth. To visibly see the secondary clusters, we created a density 0.02 deg/px map (Figure 1), by subdividing to the CDA data into 0.02-degree bins and coloring them relative to three diameter ranges using red, blue, and green bands.

Initial visual inspection of the spatial crater density map alludes to many NE-SW and NW-SE features that exhibit long ray-like shapes. These are clusters of small craters ~50m-100m in diameter (~yellow-green features in the density map, Figure 1), indicating a dominance of secondary craters. Some of these features come close to crosscutting the Chang'E 5 landing site (yellow star, Figure 1). What becomes apparent is the complexity of the cratering patterns, when only analyzing small craters (<1km). Large regions of the map have.

Conclusion: Using an automated crater detection algorithm as a tool to aid in mapping and identifying secondary crater clusters offers a quick and in-depth way to outline high-density regions of potential secondary craters. By linking secondaries to primary impacts, we can help in understanding the extent lunar material transportation across different regions. This type of analysis can quickly be achieved for large image datasets and applied to multiple sites across the Moon, increasing the scope of identify secondary craters clusters across the lunar surface.

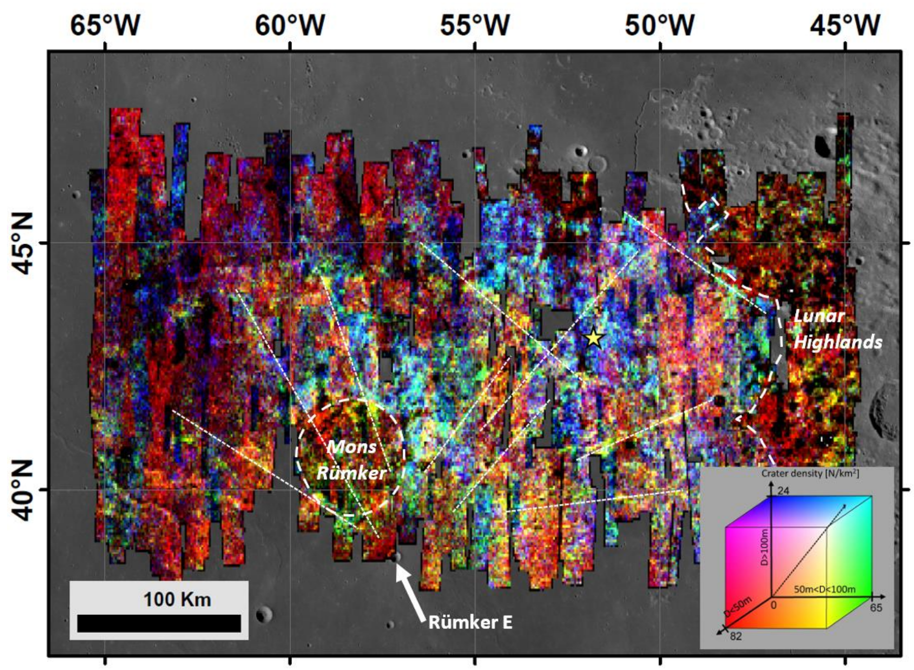

Figure 1: Spatial crater density map of the northern Oceanus Procellarum and Change'E 5 landing site (yellow star). The resolution is 0.02 px/degree, and colors indicate crater densities of specific diameter ranges (red: D<50m, green: 50 m < D < 100 m, and blue: D>100m). The map is made from 3.9 million detections on a mosaic made from 871 individual NAC images. White dashed line denotes some of the identified secondary rays/clusters, and major geological boundaries. The gaps within the mosaic were where no NAC images with favourable lighting are situated, so were not processes into a mosaic. Background image is the global LRO-WAC mosaic [14].

Acknowledgments: This work is supported by the resources provided by the Pawsey Supercomputing Centre with funding from the Australian Government, Curtin University, and the Government of Western Australia.

References: [1] Papike, J., et al. (1998). Planetary Materials. Chapter 5, 719-952. [2] Che, X., et al. (2021). Science. 374(6569), 887-890. [3] Qian, Y., et al. (2021). Earth and PLanetary Science Letters. 561, 116855. [4] McEwen, A., and Bierhaus, E. (2006). Annual Review of Earth and Planetary Sciences. [5] Lagain, A., et al. (2021). Nature Communications. 12(1), 6352. [6] Dundas, C., and McEwen, A. (2007). Icarus. 186(1), 31-40.

[7] Robinson, M.S., et al. (2010). Space Science Reviews. 150, 81–124.[8] Redmon, J., Farhadi, A. (2018). Cornell University. arXiv:1804.02767.[9]https://isis.astrogeology.usgs.gov/. [10] Benedix, G.K., et al. (2020). Earth and Space Science. 7(3), 2333-5084. [11] Lagain, A., et al. (2021). Earth and Space Science.. 8(2), 2333-5084. [12] Fairweather, J.H., et al. (2022). Earth and Space Secience. in review. [13] Fairweather, J.H., et al. (2021). 52nd LPSC. 2548, 1404. [14]https://astrogeology.usgs.gov/search/map/Moon/LRO/LROC_WAC/Lunar_LRO_LROC-WAC_Mosaic_global_100m_June2013.